Status and perspectives of the Euclid mission

Author: Alessandro Renzi (INFN Padova)

On Behalf of the Euclid Consortium

The European Physical Society Conference on High Energy Physics (EPS-HEP)
Ghent, Belgium, 10-17/07/2019

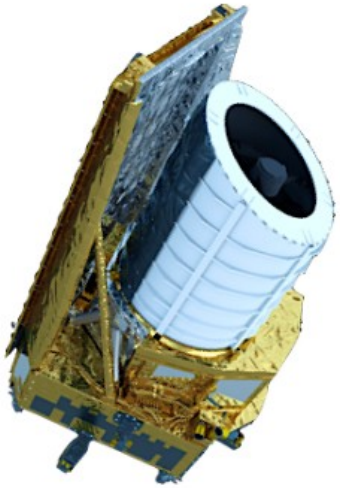

Outline

- **The Dark Universe**
  - The cosmological questions behind the Euclid experiment
- **Euclid Mission: Hardware status and perspective**
  - How the Euclid experiment will answer: how to extract the cosmological information
- **Euclid Mission: Data status and perspective**
  - How the Euclid experiment will answer: how to analyze the extracted information
- **A focus on some particular aspect of the Euclid analysis**
  - Power Spectrum, CMB Cross-Correlation and Voids
- **The years to come of the Euclid Mission**
  - Expected results and foreseen precision and accuracy

The Dark Universe

We do not know the 95% of content of the Universe

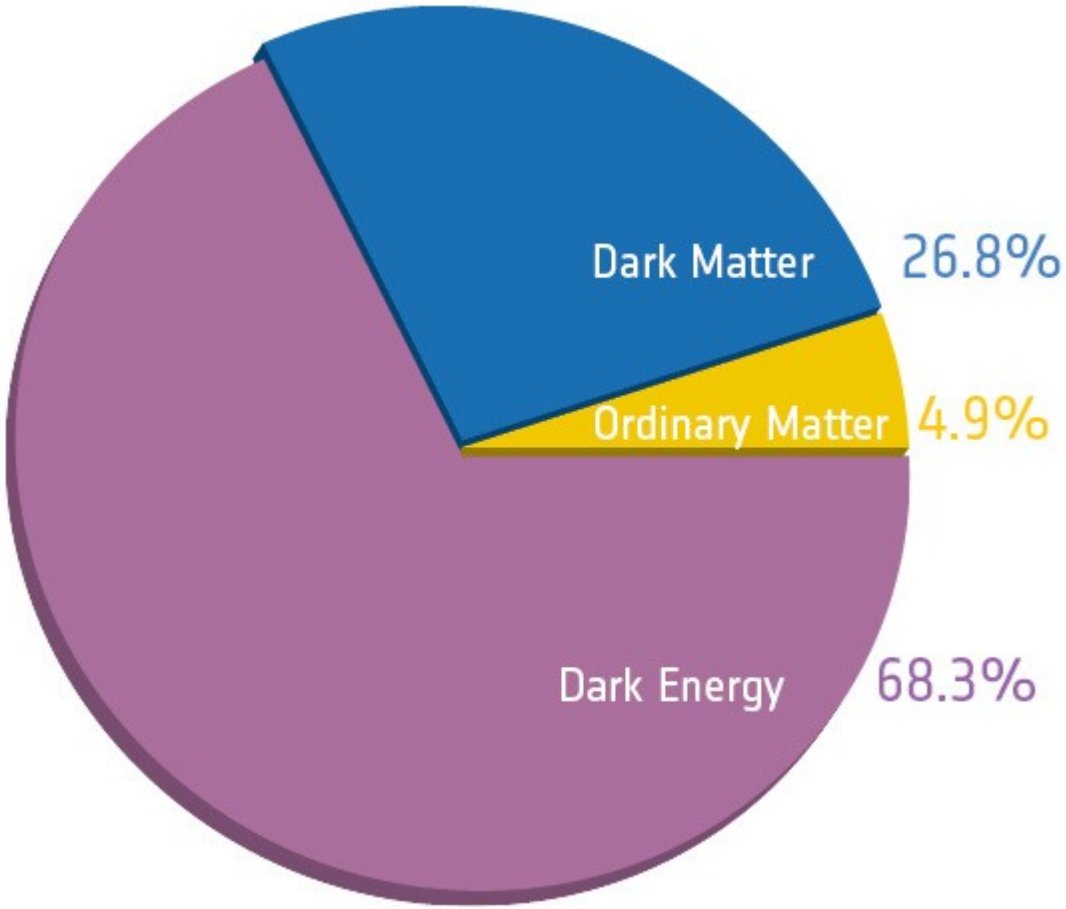

Source: ESA and the Planck Collaboration

Dark Energy

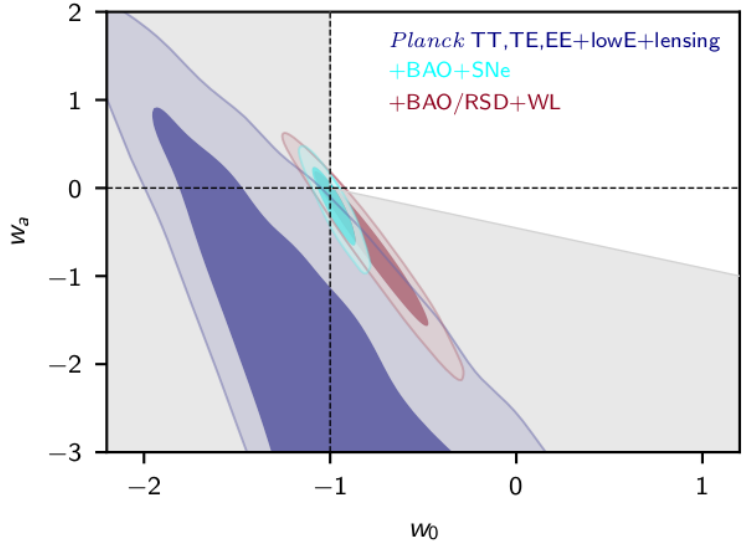

Fig. 30. Marginalized posterior distributions of the (w_0, w_a) parameters for various data combinations. The tightest constraints come from the combination *Planck* TT,TE,EE+lowE +lensing+SNe+BAO and are compatible with ΛCDM. Using *Planck* TT,TE,EE+lowE+lensing alone is considerably less constraining and allows for an area in parameter space that corresponds to large values of the Hubble constant (as already discussed in Planck Collaboration XIII 2016 and PDE15). The dashed lines indicate the point corresponding to the ΛCDM model. The parametric equation of state given by Eq. (49) stays out of the phantom regime (i.e., has $w \geq -1$) at all times only in the (upper-right) unshaded region.

$$w(a) = w_0 + (1 - a)w_a$$

Table 6. Marginalized values and 68 % confidence limits for cosmological parameters obtained by combining *Planck* TT,TE,EE +lowE+lensing with other data sets, assuming the (w_0, w_a) parameterization of $w(a)$ given by Eq. (49). The $\Delta\chi^2$ values for best fits are computed with respect to the ΛCDM best fits computed from the corresponding data set combination.

Parameter	*Planck*+SNe+BAO	*Planck*+BAO/RSD+WL
w_0	-0.961 ± 0.077	-0.76 ± 0.20
w_a	$-0.28^{+0.31}_{-0.27}$	$-0.72^{+0.62}_{-0.54}$
H_0 [km s^{-1}Mpc^{-1}]	68.34 ± 0.83	66.3 ± 1.8
σ_8	0.821 ± 0.011	$0.800^{+0.015}_{-0.017}$
S_8	0.829 ± 0.011	0.832 ± 0.013
$\Delta\chi^2$	-1.4	-1.4

Source: Planck Collaboration - Planck 2018 results. VI. Cosmological parameters

Dark Matter

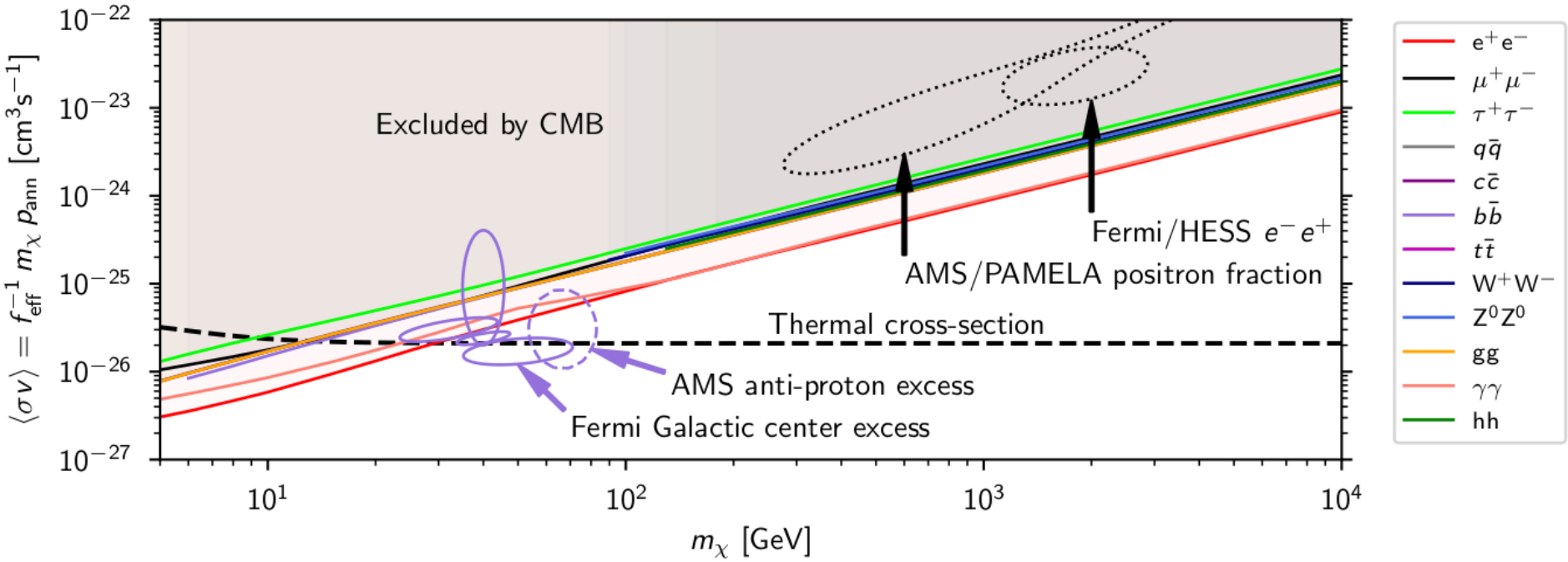

Fig. 46. *Planck* 2018 constraints on DM mass and annihilation cross-section. Solid straight lines show joint CMB constraints on several annihilation channels (plotted using different colours), based on $p_{\rm ann} < 3.2 \times 10^{-28}\,{\rm cm}^3\,{\rm s}^{-1}\,{\rm GeV}^{-1}$. We also show the $2\,\sigma$ preferred region suggested by the AMS proton excess (dashed ellipse) and the *Fermi* Galactic centre excess according to four possible models with references given in the text (solid ellipses), all of them computed under the assumption of annihilation into $b\bar{b}$ (for other channels the ellipses would move almost tangentially to the CMB bounds). We additionally show the $2\,\sigma$ preferred region suggested by the AMS/PAMELA positron fraction and *Fermi*/H.E.S.S. electron and positron fluxes for the leptophilic $\mu^+\mu^-$ channel (dotted contours). Assuming a standard WIMP-decoupling scenario, the correct value of the relic DM abundance is obtained for a "thermal cross-section" given as a function of the mass by the black dashed line.

Source: Planck Collaboration - Planck 2018 results. VI. Cosmological parameters

Neutrino

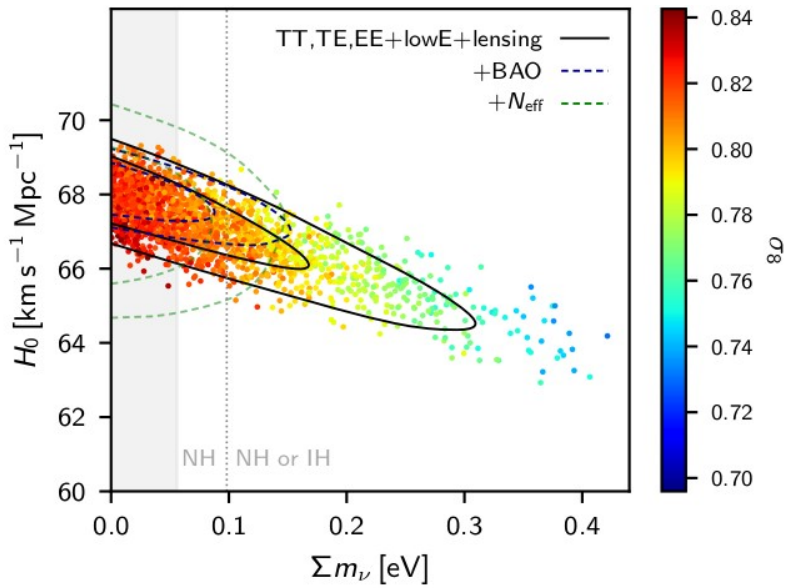

Fig. 34. Samples from *Planck* TT,TE,EE+lowE chains in the $\sum m_\nu$–H_0 plane, colour-coded by σ_8. Solid black contours show the constraints from *Planck* TT,TE,EE+lowE+lensing, while dashed blue lines show the joint constraint from *Planck* TT,TE,EE+lowE+lensing+BAO, and the dashed green lines additionally marginalize over $N_{\rm eff}$. The grey band on the left shows the region with $\sum m_\nu < 0.056$ eV ruled out by neutrino oscillation experiments. Mass splittings observed in neutrino oscillation experiments also imply that the region left of the dotted vertical line can only be a normal hierarchy (NH), while the region to the right could be either the normal hierarchy or an inverted hierarchy (IH).

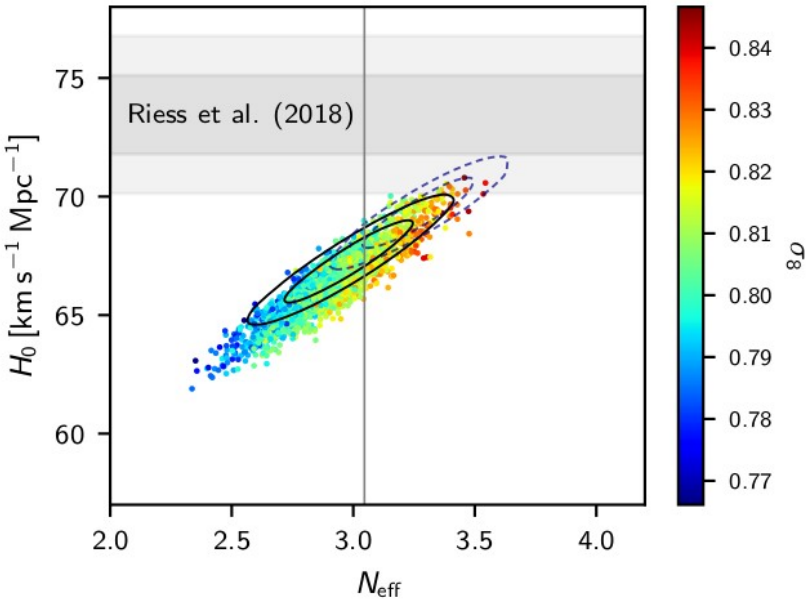

Fig. 35. Samples from *Planck* TT,TE,EE+lowE chains in the $N_{\rm eff}$–H_0 plane, colour-coded by σ_8. The grey bands show the local Hubble parameter measurement $H_0 = (73.45 \pm 1.66)$ km s^{-1}Mpc^{-1} from Riess et al. (2018a). Solid black contours show the constraints from *Planck* TT,TE,EE +lowE+lensing+BAO, while dashed lines the joint constraint also including Riess et al. (2018a). Models with $N_{\rm eff} < 3.046$ (left of the solid vertical line) require photon heating after neutrino decoupling or incomplete thermalization.

Source: Planck Collaboration - Planck 2018 results. VI. Cosmological parameters

Modified Gravity

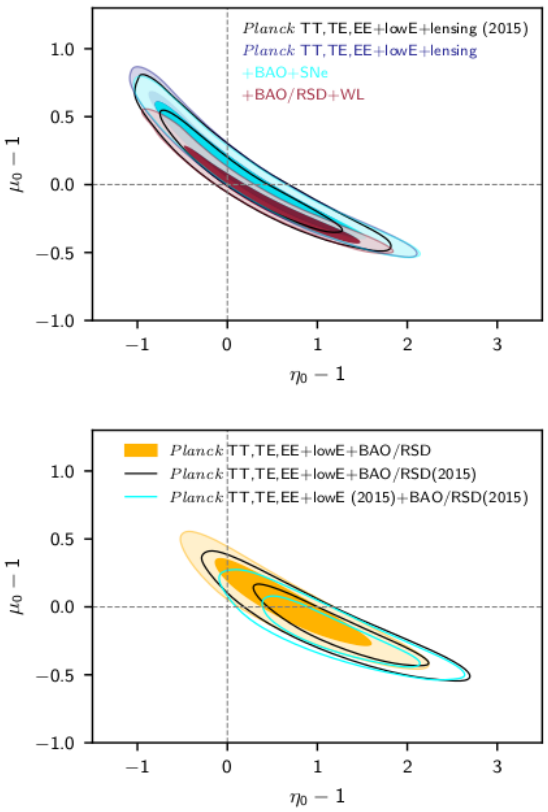

Fig. 31. *Top*: Marginalized posterior distributions of the MG parameters μ and η for *Planck* TT,TE,EE+lowE+lensing data alone and in combination with external data (as indicated in the legend), using the late-time parameterization and neglecting any scale dependence. The dashed lines show the standard ΛCDM model. *Bottom*: Impact of the BAO/RSD and *Planck* TT,TE,EE +lowE data, compared to the 2015 results. For the 2018 *Planck* data, the contours shift towards lower values of $\eta_0 - 1$, along the maximum degeneracy line (black versus cyan contours) and shift in the same direction when using the BAO/RSD data (yellow versus black contours).

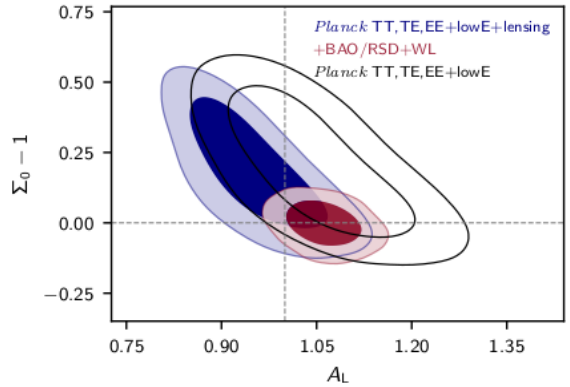

Fig. 32. Degeneracy between A_L and $\Sigma_0 - 1$, computed as a derived parameter in our (μ, η) parameterization. The horizontal dashed line includes ΛCDM (but is also marginalized over one of the two degrees of freedom in the μ–η space). The vertical dashed line shows $A_L = 1$. The filled contours use the *Planck* TT,TE,EE+lowE+lensing likelihood, alone and in combination with WL+BAO/RSD data. The unfilled contours show the constraints from *Planck* TT,TE,EE+lowE. Note that A_L only affects CMB lensing of the *Planck* power spectra by definition, as discussed in Sect. 6.2.

$$ds^2 = (1+2\Psi)dt^2 - a(t)^2(1+2\Phi)dx^2$$

μ, η and Σ are MG fenomenological parameters

μ → modification of the Poisson equation (for Ψ)

η → additional anisotropic stress ($\Psi \neq \Phi$)

Σ → deviations of the lensing potential from the GR prediction

Source: Planck Collaboration - Planck 2018 results. VI. Cosmological parameters

The Euclid Mission

The Euclid Consortium

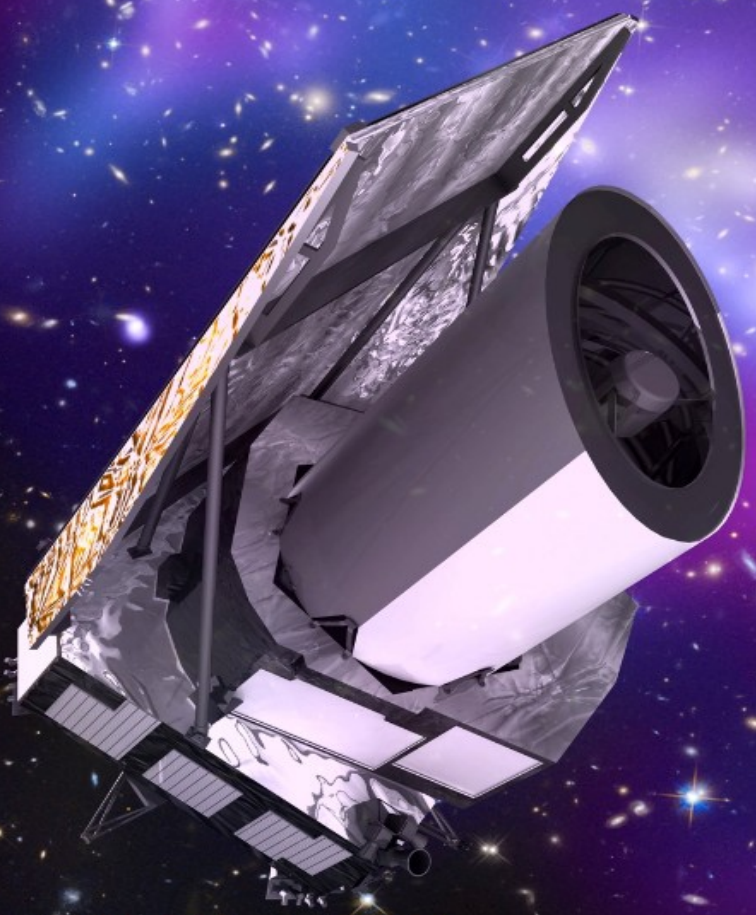

An artist view of the Euclid satellite – courtesy ESA

- 16 countries +
- More than 120 institutes/labs
- More than 1200 members

www.euclid-ec.org
sci.esa.int/euclid

July 2017 - Rencontres du Vietnam

L. Valenziano on behalf of the EC

The Euclid Satellite

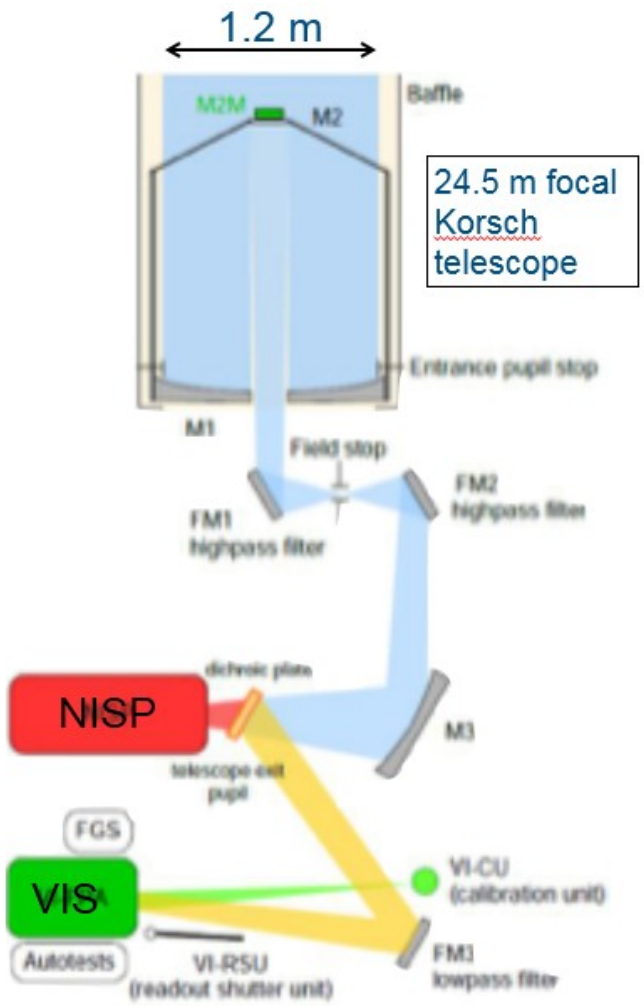

- **FoV**: 0.787 x 0.709 = 0.557 deg^2
- **Active area**: 877 cm^2
- **Detectors**: 6 x 6 e2v CCDs
- **Plate scale**: 0.1 arcsec/pix
- **609 megapixel** visible camera
- **Spectral range**: 550–920nm
- **Data-rate**: ≤ 520 Gbits/day

(M. Cropper & VIS Team)

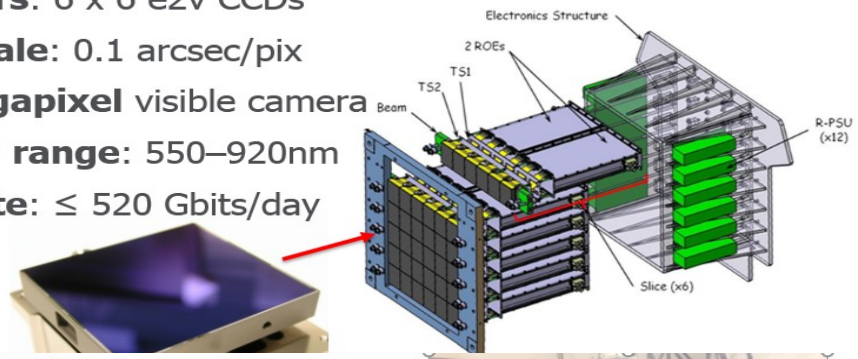

(T. Maciaszek, A. Ealet & NISP Team)

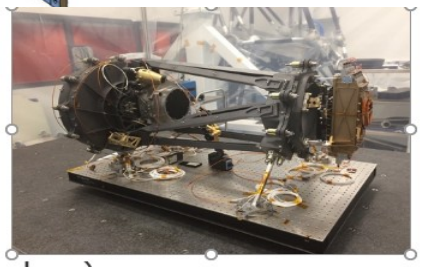

- **FoV**: 0.55 deg^2
- **Mass**: 158 Kg
- **Telemetry**: < 290Gb/day
- **Size**: 1m x 0.5m x 0.5m
- **IR detectors**: 16x 2Kx2K H2RG (Teledyne)
- **Plate scale**: 0.3 arcsec/pix
- **3 Filters:**
  Y (950-1192nm)
  J (1192-1544nm)
  H (1544-2000nm)
- **4 Grisms**:
  1B (920-1300), 1 orient. 0^0
  3R (1250-1850), 3 orient. 0^0,90^0,180^0

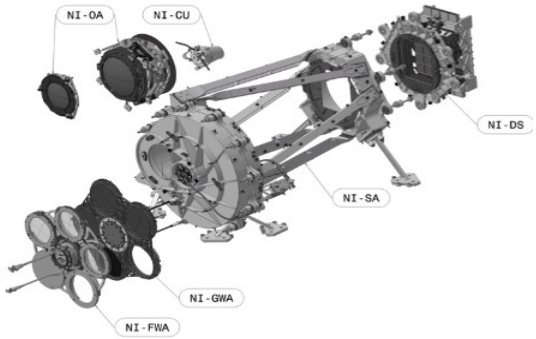

VIS – Visible InStrument

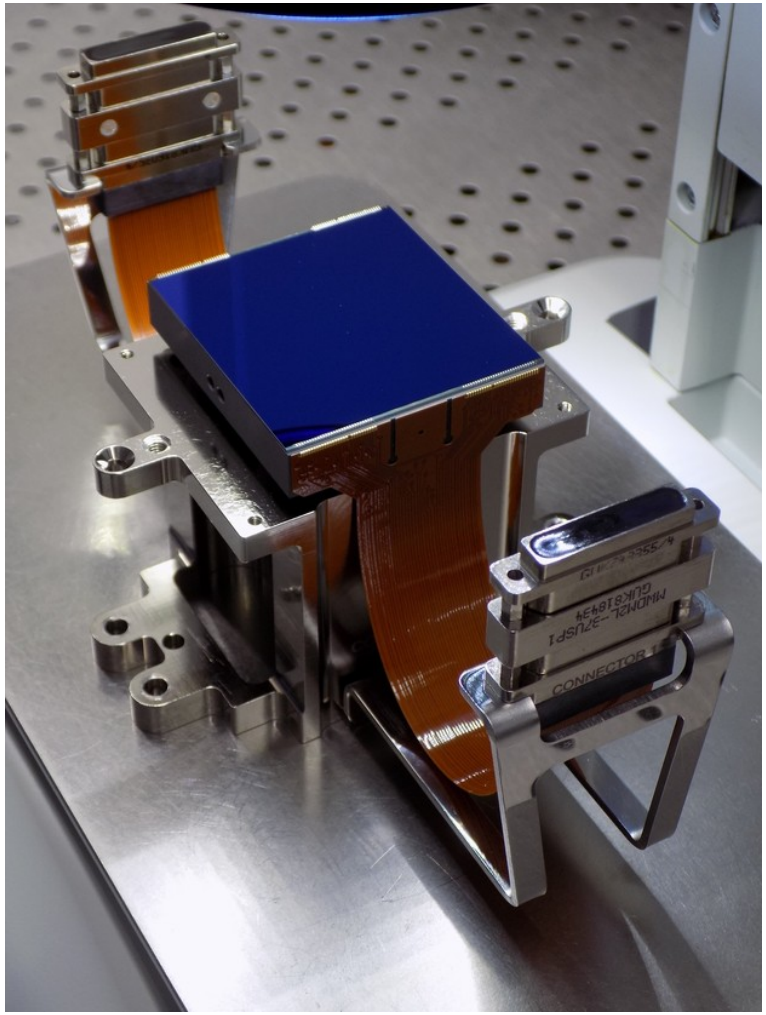

Euclid VIS CCD

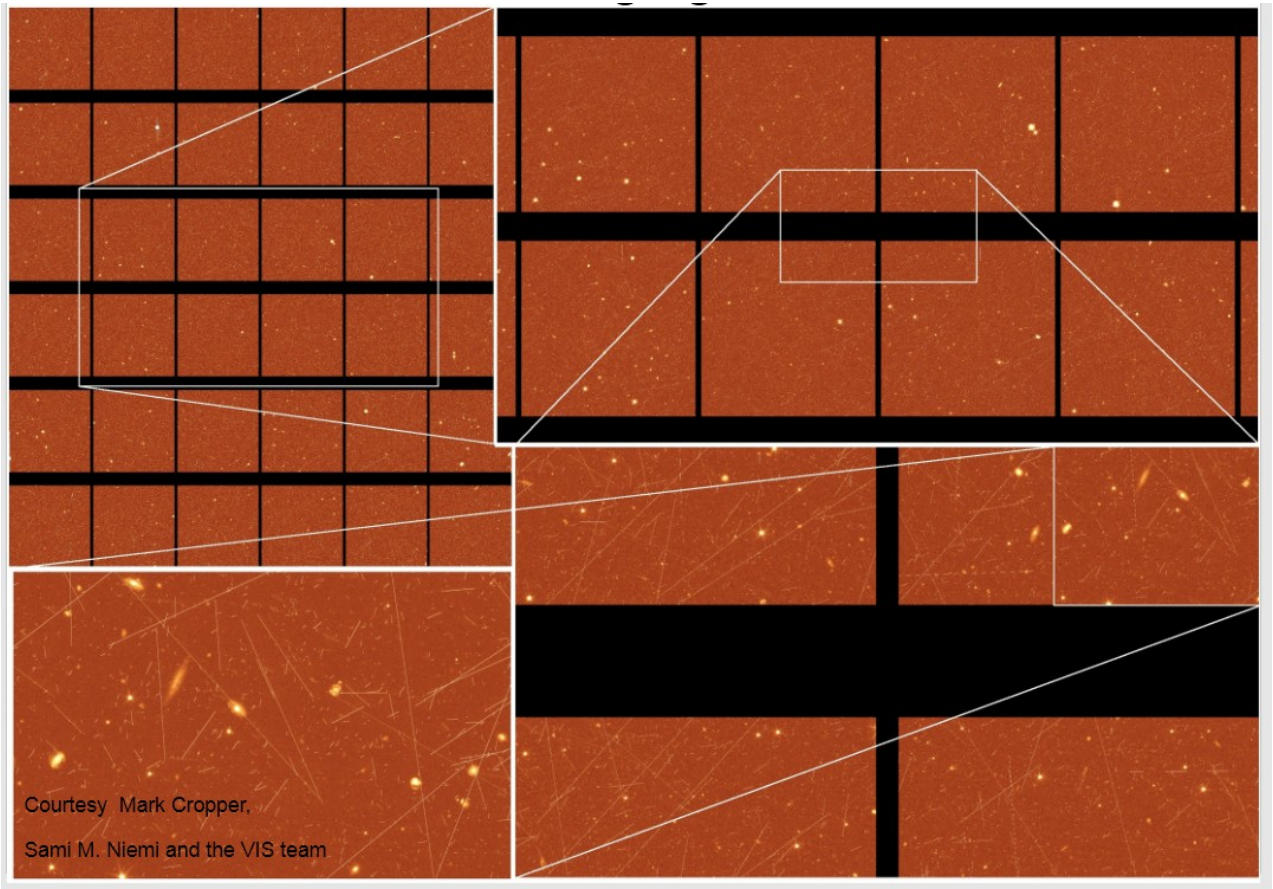

VIS - Data

VIS → Shapes of galaxies → weak lensing

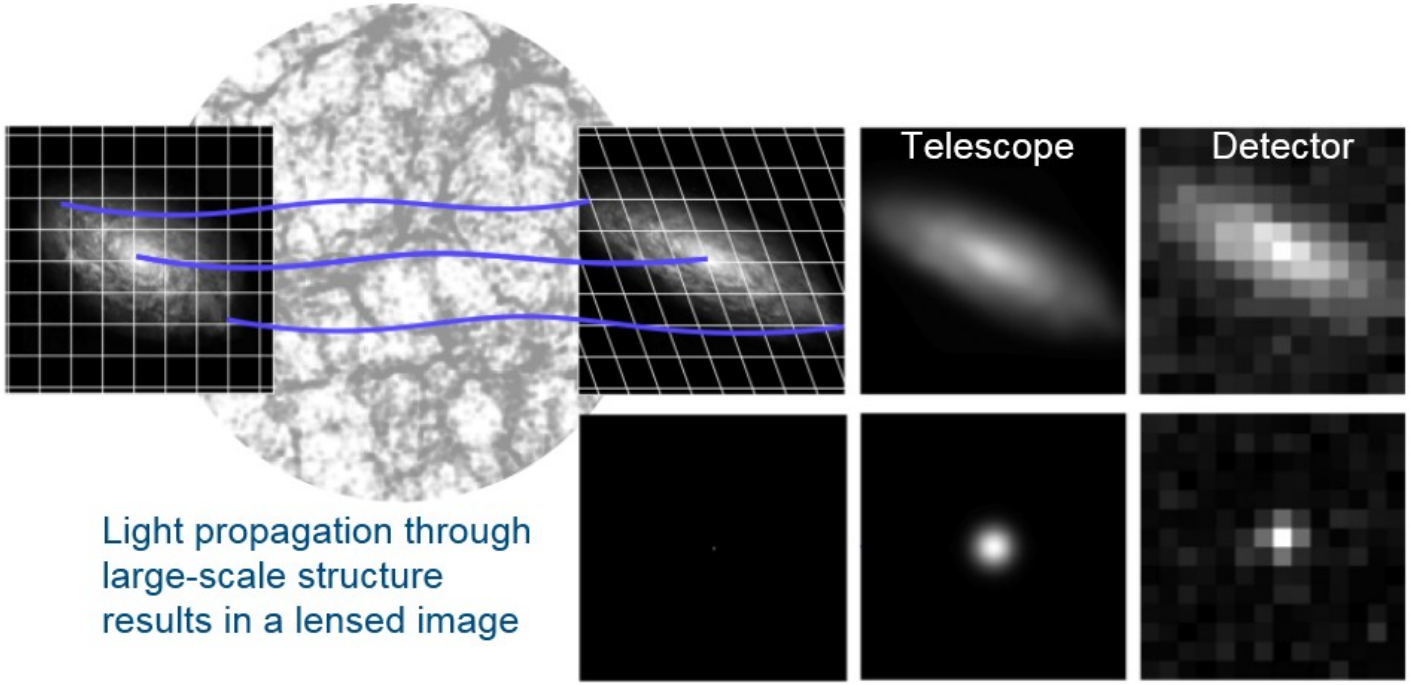

NISP – Near Infrared SpectroPhotometer

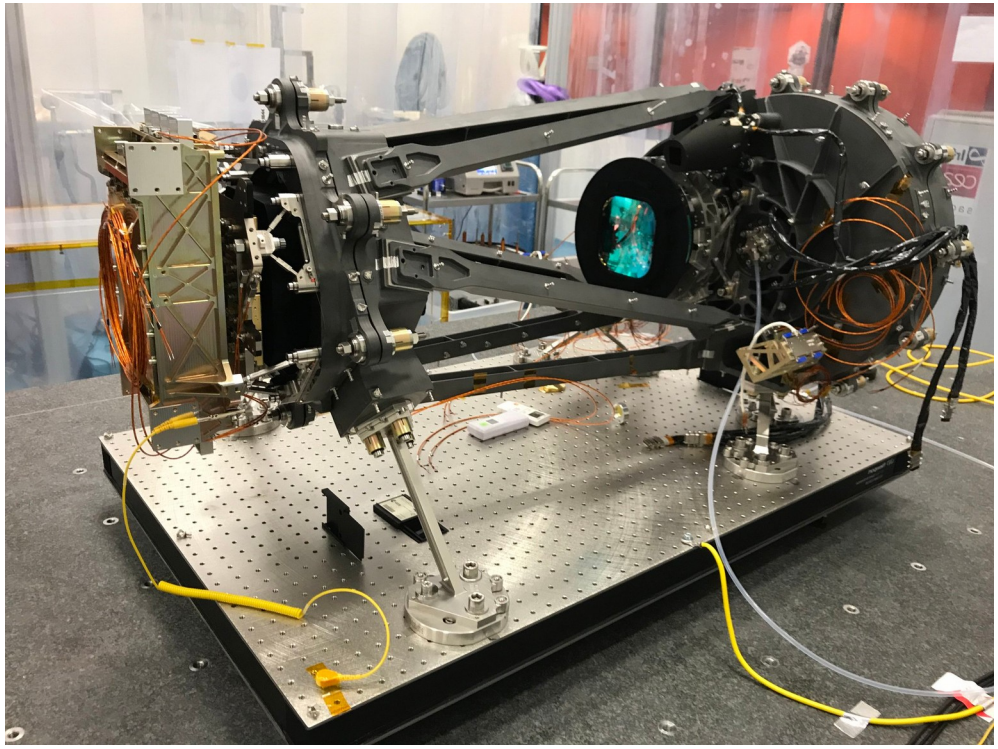

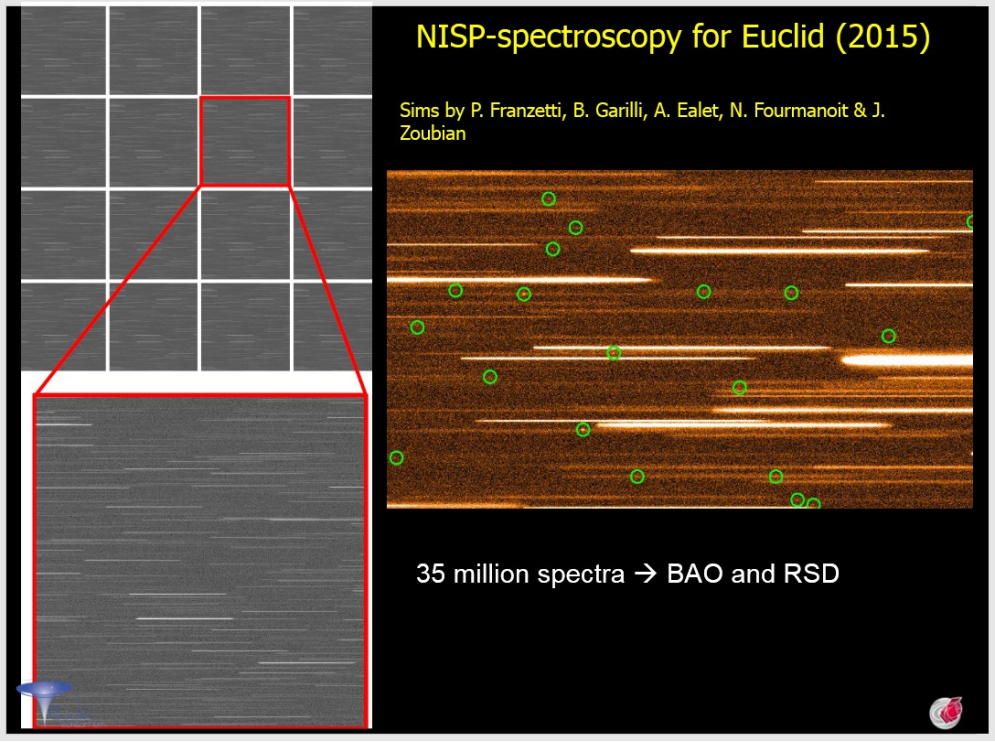

NISP - Data

NISP → Redshifts → Redshift Space Distrortions (RSD) and Barionic Acoustic Oscillations (BAO)

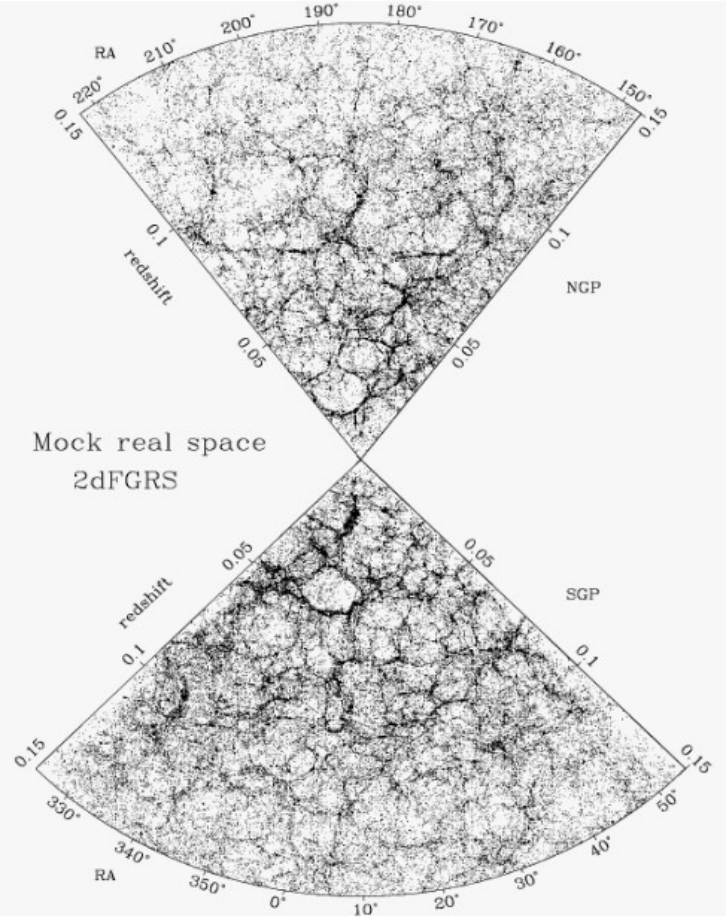

Focus on some analysis

Galaxy Clustering Power Spectrum

Power Spectrum Estimation is the basis of many cosmological analisys linking theory and data

$$< \rho(\mathbf{k})\rho(\mathbf{k}') > \propto \mathbf{P}(\mathbf{k})\delta^{\mathbf{Dirac}}(\mathbf{k}-\mathbf{k}')$$

Due to its importance, the Euclid collaboration is working to provide a robust and reliable power spectrum estimator code to be used by the collaboration (e.g. for likelihood analysis)

Window Function (Fourier and Eperimental)

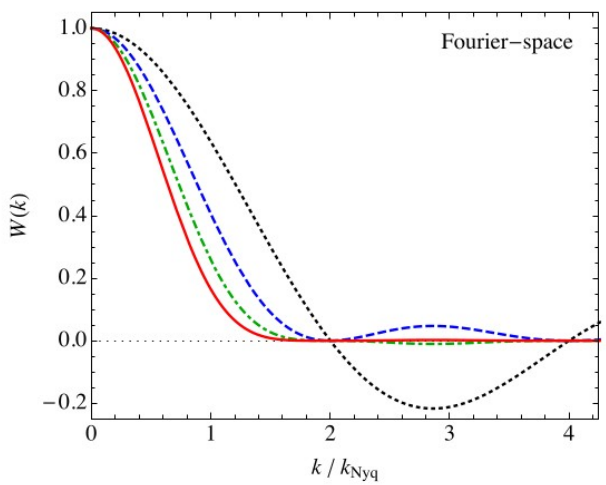

Interlacing (Fourier Transform errors)

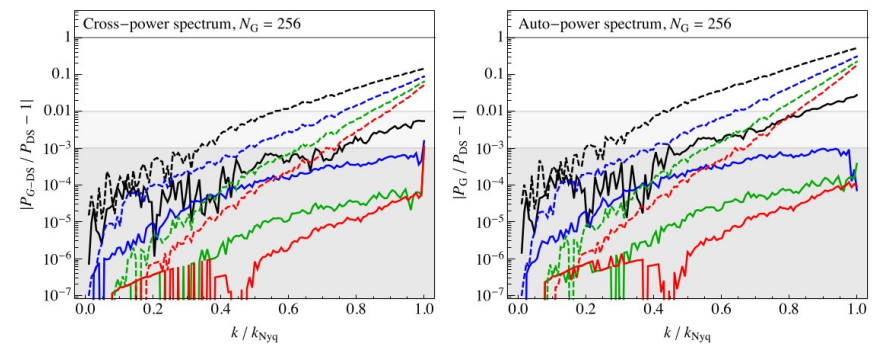

Relation to theory

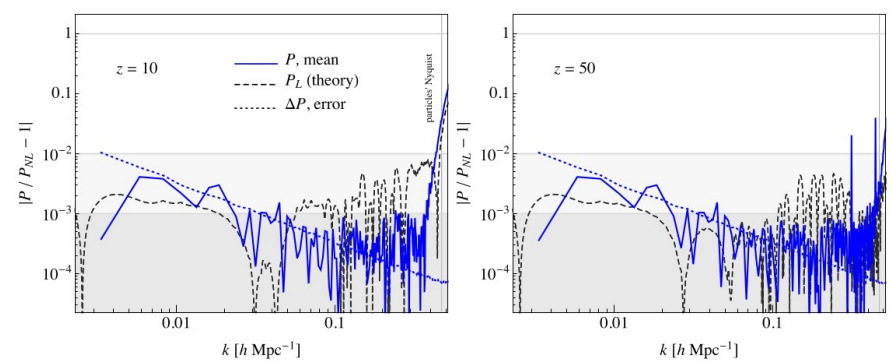

Plots from: Sefusatti et al. MNRAS 460, 3624–3636 (2016)

CMB-LSS Cross-Correlation

Cross-Correlation can improve the precision and accuracy of experimental results:

- Precision: more than one dataset used to estimate the same quantities
- Accuracy: different systematics (both physical and instrumental) improve the general robustness of the results

Planck Lensing (red) vs Hearchel galaxy (blu) data

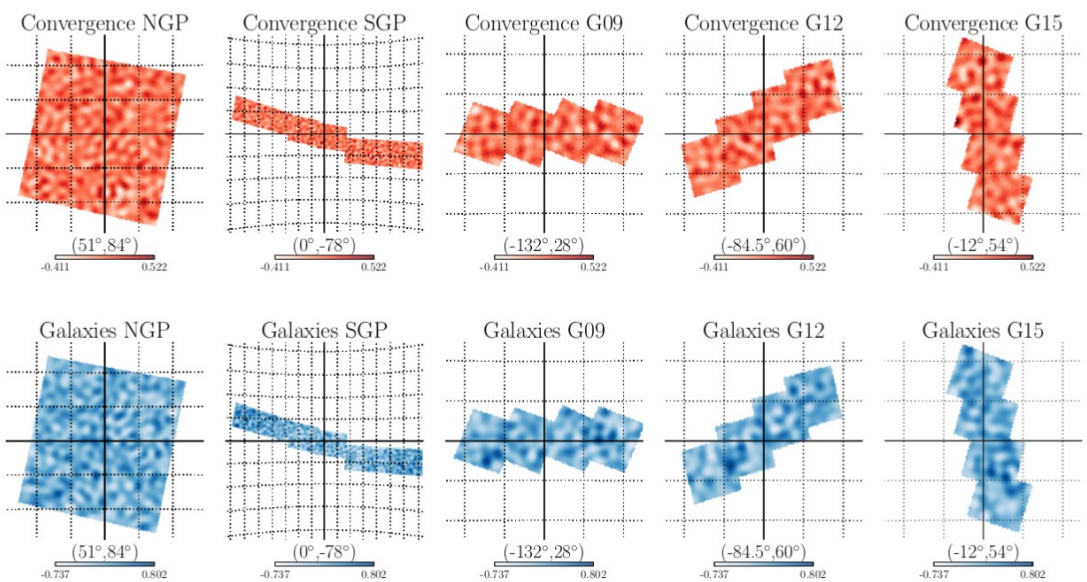

Figure 5. Convergence maps (upper row) and galaxy overdensity maps (lower row) in the H-ATLAS fields: multipoles $\ell > 400$ for which $(S/N)_\ell \lesssim 0.3$ have been filtered out. Galactic longitude and latitude (l, b) of patch centers are provided in brackets. The grid overlay has spacing of 3° in each box.

Cross-correlation power spectrum

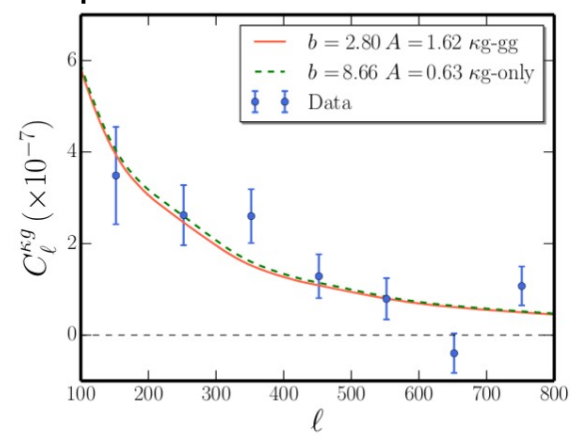

Figure 7. The CMB convergence-galaxy density cross-spectrum as measured from Planck and *Herschel* data. The data points are shown in blue, with error bars computed using the full covariance matrix obtained from Monte Carlo realizations of convergence maps. The theoretical spectra calculated with the bias values inferred from the likelihood analysis (as described in text) using the cross-correlation data only (solid red line) and the cross-correlation together with the galaxy autocorrelation data (dot-dashed green line) are also shown; we fix $\alpha = 3$ in this analysis. The null (no correlation) hypothesis is rejected at the $20\,\sigma$ level.

Plots from: Bianchini et al. ApJ 802 64 (2015)

Voids

Studying the underdense region of the universe (called Voids) can allow estimate the same quantities as in “standard” analysis with a largely independed semple of data.

Voids can be analysed as stand-alone dataset or cross-correlated with any other dataset that traces the same quantities of interest

Voids identification algotithm(s)

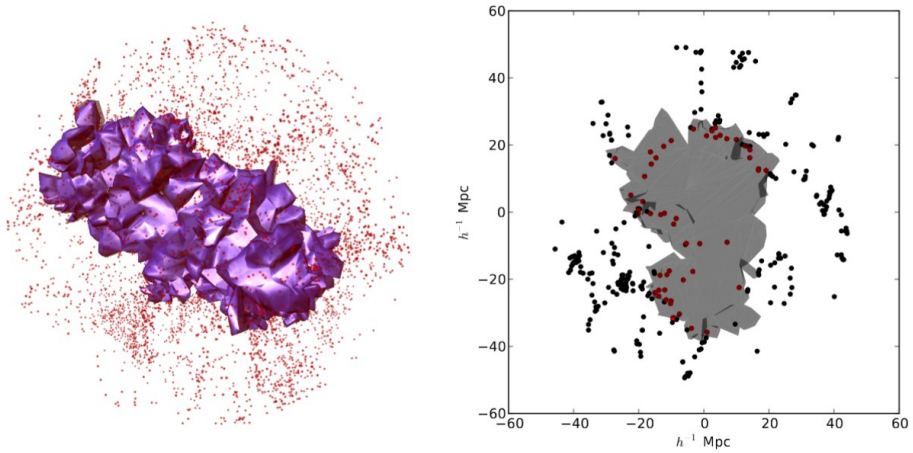

FIG. 2.— *Example Voronoi-based void.* We show the Voronoi cells that define the void in purple with galaxies in red (left). Shown is a void with effective radius 20 h^{-1}Mpc within a spherical region of radius 50 h^{-1}Mpc. Galaxy point sizes are proportional to their distance from the point of view. Galaxies interior to the void are shaded dark red. On the right is a 5 h^{-1}Mpc thick slice through the same void, showing exterior galaxies in black and interior galaxies in red. The orientation of the void is different between the panels to highlight different aspects of the structure.

Plots from: Sutter et al. ApJ 761, 44 (2012)

Simulations vs theory

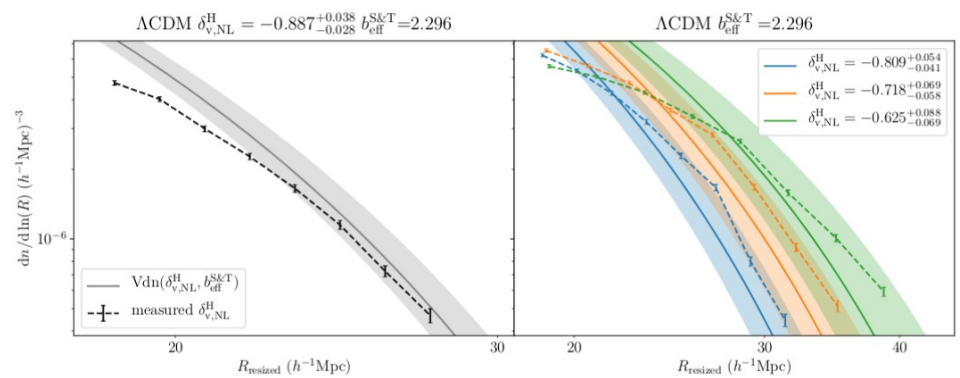

Figure 3: Match of the measured abundances of voids (after resizing procedure) with theoretical predictions. The left panel shows the measurement for $\delta^{H}_{v,NL} = -0.887$ (black curve), and the corresponding theoretical void size function obtained using b_{eff} as described in the text (grey curve). The right panel shows the measured void abundances for various thresholds $\delta^{H}_{v,NL}$ (dashed curves), and the corresponding theoretical void size functions (solid curves). The current resized voids correspond to observable voids in the range $R_{eff} = [35 - 70]$ h^{-1}Mpc. Shaded areas give the uncertainty in the resizing procedure (see text).

Plots from: Verza et al. arXiv:1906.00409 (2019)

Expected Results

Euclid Timeline for data release and analysis

Launch Date: June 2022

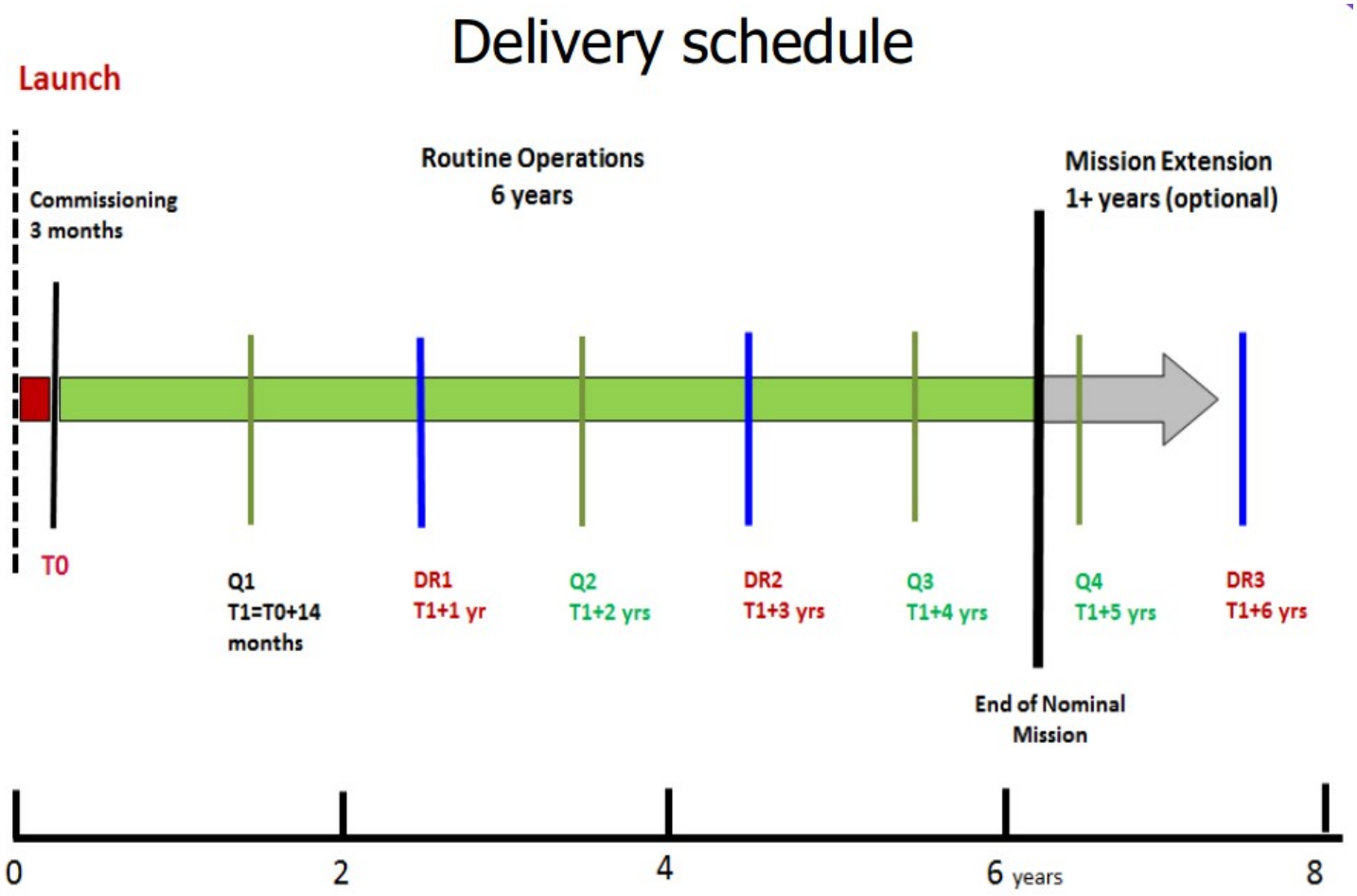

Euclid Weak Lensing expected performances

Euclid WL predicted performances

Euclid Consortium

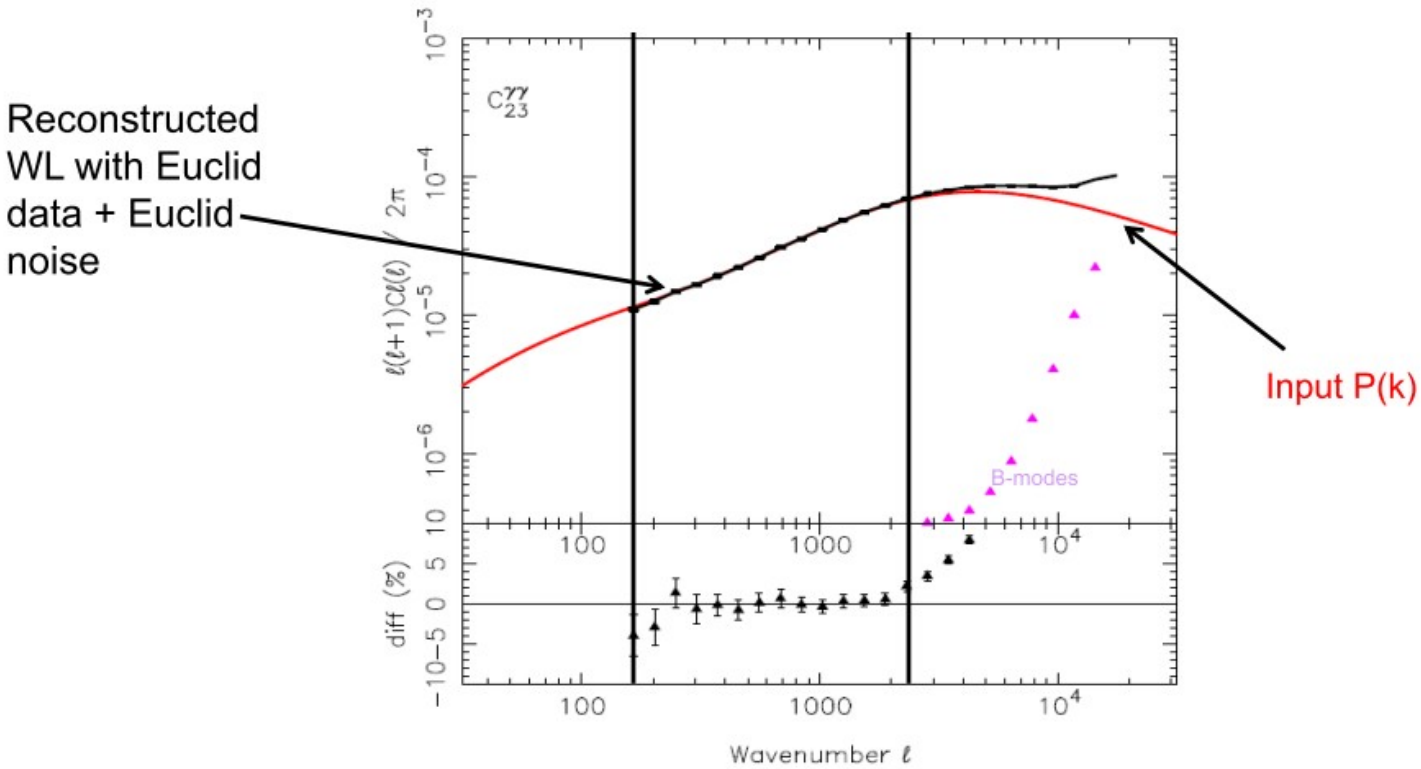

Tomographic WL shear cross-power spectrum for 0.5 < z < 1.0 and 1.0 < z < 1.5 bins.
Percentage difference [expected – measured] power spectrum: recovered to 1% .

Euclid Deep Surveys -Valencia March 29-30, 2012

Euclid P(k) expected performances

Euclid GC predicted performances

Euclid Consortium

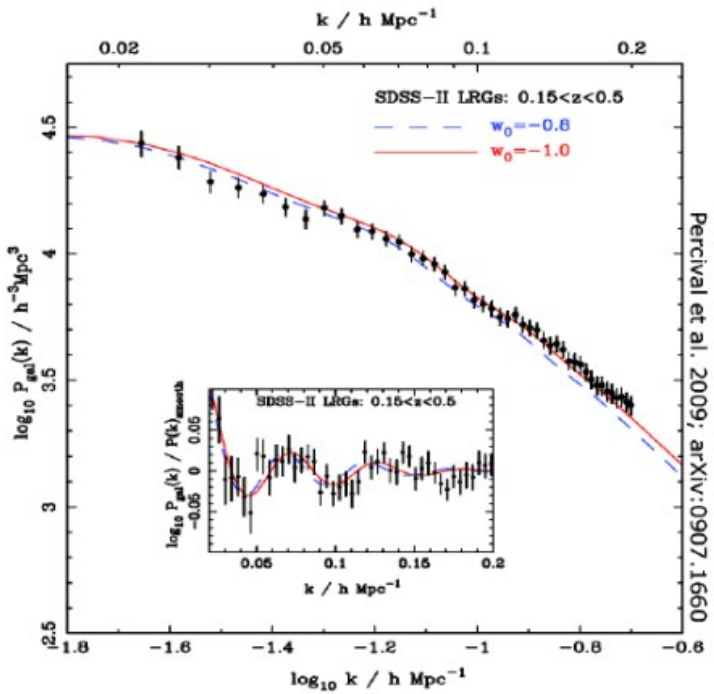

Percival et al. 2009; arXiv:0907.1660

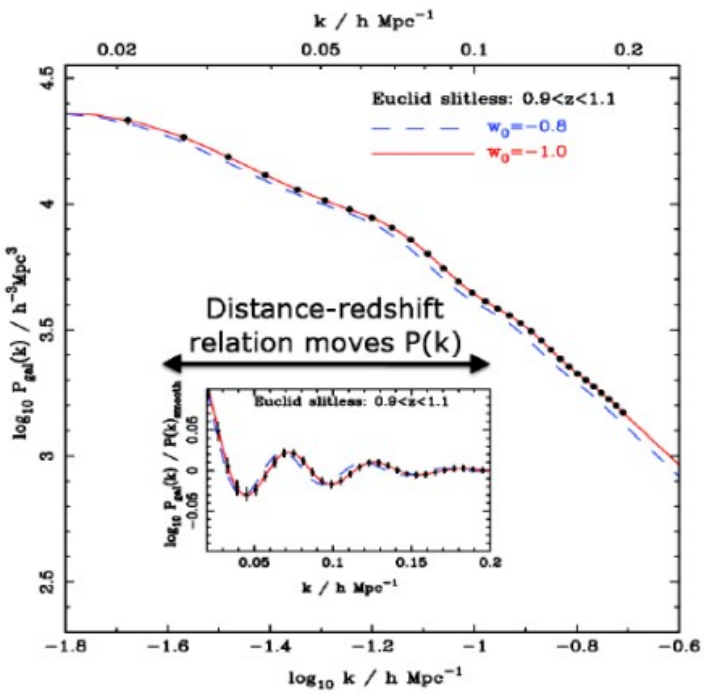

SDSS-II LRG galaxies - Euclid

Percentage difference [expected – measured] power spectrum: recovered to 1% .

Euclid Deep Surveys -Valencia March 29-30, 2012

Euclid Expected Paramaters Accuracy

Ref: Euclid RB arXiv:1110.3193

	Modified Gravity	Dark Matter	Initial Conditions	Dark Energy		
Parameter	γ	m_ν /eV	f_{NL}	w_p	w_a	*FoM*
Euclid primary (WL+GC)	0.010	0.027	5.5	0.015	0.150	$= 1/(\Delta w_0 \times \Delta w_a)$ 430
EuclidAll (clusters,ISW)	**0.009**	**0.020**	**2.0**	**0.013**	**0.048**	**1540**
Euclid+Planck	0.007	0.019	2.0	0.007	0.035	4020 → **6000**
Reference (2011)	0.200	0.580	100	0.100	1.500	~10
Improvement Factor	**30**	**30**	**50**	**>10**	**>40**	**>400**

Soon an improved table of forecasted error accuracy will come out

Ending Slide

Thanks for your attention

AR wishes to thank Y. Mellier, G. Guzzo, B. Granett, E. Branchini, J-C Salvignol, ADS and TAS-I for useful material.